Eur. Phys. J. AP **6**, 81–87 (1999)

THE EUROPEAN PHYSICAL JOURNAL APPLIED PHYSICS

Multiple light scattering in random systems: Analysis of the backscattering spot image

A. Arhaliass[1,a] and P. Snabre[2]

[1] Université de Technologie de Compiègne, Département Génie Chimique, B.P. 649, 60206 Compiègne, France
[2] Institut de Sciences et de Génie des Matériaux et Procédés, B.P. 5, 66120 Font Romeu, France

Received: 5 May 1998 / Revised: 5 November 1998 / Accepted: 23 December 1998

Abstract. This study concerns the multiple scattering of light in random granular systems and the analysis of the image formed by the light scattered by a random medium. We developed an imagery method with high grey level resolution for visualization and analysis of the intensity profile in the backscattering spot image. We further present statistical models for the radiative transfer in granular media only involving the photon mean path length, the asymmetry factor and the absorption probability of photons. A renormalization of the photon trajectory in the medium gives a photon transport equation for anisotropic scattering and leads to an analytical expression for the intensity profile in the backscattering spot. We finally compare the results from imagery experiments with the predictions from numerical simulations and statistical models.

Résumé. Ce travail concerne la diffusion multiple de la lumière dans les systèmes dispersés aléatoires et la caractérisation du milieu par analyse de la tache de rétrodiffusion. Nous avons mis au point une technique d'imagerie à haute résolution en niveaux de gris pour la visualisation et l'analyse du profil de luminosité dans la tache de rétrodiffusion. Nous présentons par ailleurs des modèles statistiques du transfert radiatif dans les milieux granulaires où interviennent seulement le libre parcours moyen, le facteur d'asymétrie et la probabilité d'absorption des photons. Dans le cas de la diffusion anisotrope, nous effectuons une renormalisation de la trajectoire des photons dans le milieu pour aboutir à une équation de transport des photons et à une expression analytique du flux lumineux dans la tache de rétrodiffusion. Nous comparons enfin les résultats des expériences d'imagerie avec les prévisions des simulations numériques et des modèles statistiques.

PACS. 07.60.-j Optical instruments, equipment, and techniques – 02.70.Lq Monte-Carlo and statistical methods - 82.70.-y Disperse systems

1 Introduction

Studies of transport phenomena in industrial reactors using particulate solids need the development of new measuring techniques for a direct evaluation of the dispersed phase properties such as particle size and concentration in the reactor. In this field, the optical techniques based on light extinction or diffuse scattering are of the first interest. These techniques generally use reflection or transmission optic fiber probes and produce on line particle size analysis [1]. However, sizing based on reflection probes is incurate unless the receiving sensor is calibrated against the material under test [2] and extinction sensors may only be applied to sufficiently dilute systems. Light propagation in dispersed media is often described through integer-differential equations of energy conservation which resolution involves complex mathematical theories [3].

The exact solutions of transfer equation are often restricted to isotropic and quasi-conservative scattering and further neglect the interferences between the wavelets scattered by elementary particles. Light scattering may be considered as independent for randomly distributed media of large particles with diameter d larger than the wavelength λ of the incident radiation (size parameter $\alpha = \pi d/\lambda > 10$) [4]. A coherent scattering peak however occurs in the vicinity of the backscattering direction $\theta = \pi$ [5] even for random suspensions of large particles, but sufficiently away from this direction, the interferences average tends to zero.

This work, concerns with the anisotropic multiple scattering of an non polarized incident light in a random suspension of large particles. We propose a sizing optical technique based on the intensity analysis of the incoherent backscattering spot image formed by the light that scattered from a gas/solid or liquid/solid random medium. For large particles, the photon mean free path is defined by the

[a] e-mail: abdellah.arhaliass@utc.fr

empirical expression of the efficiency factor Q_s giving the energy scattered per unit volume [4]:

$$Q_s = 2 + 0.5\alpha^{-8/9}. \quad (1)$$

For large particles $Q_s = 2$, the photon mean path length can be expressed as a function of the scattering cross-section σ_s:

$$\lambda = \frac{2}{\sigma_s} \cdot \quad (2)$$

Large nonspherical particles with random orientation scatter light in a way similar to equivalent area spheres [4]. Therefore we may consider multiple light scattering as a diffusive process at interfaces (diffusion approximation) and substitute the scattering cross-section in (2) by the particle area σ per unit volume [6], which gives:

$$\lambda = \frac{2}{\sigma} = \frac{d}{3\phi} \quad (3)$$

where ϕ is the particle volume fraction and d the diameter of spheres. In the case of polydispersed particles, the surface area then takes the form $\sigma = 6\phi\langle 1/d\rangle$ where the bracket denotes the average over the collection of scattering centers. The light scattered by large particles is forward peaked. The anisotropic scattering of light by an elementary large particle can be characterized by the anisotropy coefficient or asymmetry factor g which is the average value of $\cos\theta$ over the phase function $\psi(\theta, \varphi)$ giving the probability of the scattering direction θ, φ ($g = 0$ for Rayleigh particles and $-1 < g < 1$ for Mie scattering) [4]

$$g = \langle\cos\theta\rangle = \frac{\displaystyle\int_{4\pi} \psi(\theta,\varphi)\cos\theta \mathrm{d}\Omega}{\displaystyle\int_{4\pi} \psi(\theta,\varphi)\mathrm{d}\Omega} \quad (4)$$

where $\mathrm{d}\Omega = \sin\theta \mathrm{d}\theta\mathrm{d}\varphi$ is an elementary solid angle. In the case of non spherical particles with random orientations, we can consider that the asymmetry factor is equivalent to the anisotropy coefficient of the equivalent area sphere. The accurate description of the scattering phenomena needs to take into account the entire phase function, especially for absorbing particles which scatter a non negligible part of the incident light in the backward direction. In this study, we separate the forward and the backward diffusion processes. Hence, we define the scattering probabilities P_A, P_B and the asymmetry factors g_A, g_B pertaining to forward and backward directions such that:

$$g_A = \langle\cos\theta\rangle_{0\le\theta\le\pi/2} = \frac{\displaystyle\int_0^{\pi/2} H(\theta)\sin\theta\cos\theta \mathrm{d}\theta}{\displaystyle\int_0^{\pi/2} H(\theta)\sin\theta \mathrm{d}\theta}$$

$$g_B = \langle\cos\theta\rangle_{\pi/2\le\theta\le\pi} = \frac{\displaystyle\int_{\pi/2}^{\pi} H(\theta)\sin\theta\cos\theta \mathrm{d}\theta}{\displaystyle\int_{\pi/2}^{\pi} H(\theta)\sin\theta \mathrm{d}\theta} \quad (5)$$

where $H(\theta) = \psi(\theta)\sin(\theta)$ is the probability density of the scattering angle θ. The mean asymmetry factor g is the given by:

$$g = g_A P_A + g_B P_B. \quad (6)$$

We further define the absorption parameter K of photons between two scattering events when particles absorb a part of the incident light. Anisotropic multiple scattering of a non-polarized radiation by a collection of large particles is presented in this paper in relation with the diffusion approximation. We have developed numerical simulations for relating the intensity profile in the backscattered spot to the physical parameters λ, g and K.

2 Numerical simulations

The comparison between imagery experiments and a representation of light diffusion in a dispersed medium by three parameters is made by simulating multiple scattering of light by a Monte-Carlo method that will be described briefly below [7]. We consider a random set of scattering centers between two parallel infinite plates separated by a distance L. The incident photons arrive in the three-dimensional medium along the direction $\theta = 0$ normal to the plane limiting the scattering volume.

Numerical simulations consist in sending photons one by one, which implies that photons cannot interfere with each other. For the numerical simulations, a random number generator first allows to compute the photon path length x between collisions according to the cumulative probability density inferred from the Beer's law $1 - \mathrm{e}^{-x/\lambda}$ and then to test if the photon is absorbed or not with respect to the absorption parameter K. A third random number determines whether the photon is scattered in the forward or backward direction with respect to the value of P_B.

We consider a uniform probability density $P(\theta) = \sin(\theta)/(1-\cos\beta)$ of forward or backward scattering directions in a cone of angle β. The asymmetry factors $g_A(\beta)$ and $g_B(\beta)$ then obey the following laws:

$$g_A(\beta) = \frac{\displaystyle\int_0^{\beta} P(\theta)\cos\theta \mathrm{d}\theta}{\displaystyle\int_0^{\beta} P(\theta)\mathrm{d}\theta} = \frac{\sin^2\beta}{2(1-\cos\beta)}$$

$$g_B(\beta) = \frac{\displaystyle\int_{\pi-\beta}^{\pi} P(\theta)\cos\theta \mathrm{d}\theta}{\displaystyle\int_{\pi-\beta}^{\pi} P(\theta)\mathrm{d}\theta} = \frac{-\sin^2\beta}{2(1-\cos\beta)} \cdot \quad (7)$$

The coordinates of the photon are then computed, step by step, by introducing the intermediate reference frame R_i in the ith diffusion step. The polar and azimuthal scattering angles $0 < \theta < \varphi$ and $0 < \beta < 2\pi$, taken with respect to R_i, are randomly sampled. The coordinates $\mathbf{W}_i$ of the

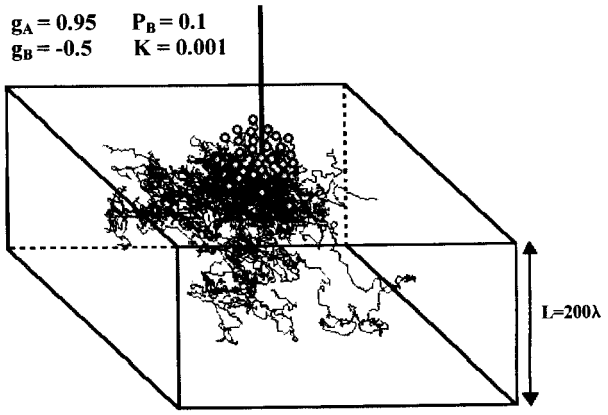

Fig. 1. Numerical simulation of the diffusive process of photon scattering in a three-dimensional random medium ($g = 0.8$), $g_A = 0.95$, $g_B = 0.1$, $P_B = 0.1$, $K = 0.001$ and $L = 200\lambda$). Grey circles indicate the backscattered photons.

photon in the laboratory reference frame then obey the recurrence relation:

$$\mathbf{W}_i = \mathbf{W}_{i-1} + \bar{\bar{Y}}_i \mathbf{U}_i \quad \text{with} \quad \bar{\bar{Y}}_i = \bar{\bar{Y}}_{i-1} \bar{\bar{X}}_i \tag{8}$$

where $\mathbf{U}_i(x, 0, 0)$ are the coordinates of the photon in the reference frame R_i, $\bar{\bar{X}}_i$ the transfer matrix from R_{i-1} to R_i and $\bar{\bar{Y}}_0$ the diagonal unity matrix. For each photon escaping from the medium, we determine the backscattering angle θ, the distance D from the incident source and the number N of scattering events. Figure 1 shows a three-dimensional simulation of photon diffusion by anisotropic scatterers. The numerical simulations then give the backscattering probability $P(D, N)$ of photons at radial distance D after N scattering events.

3 Statistical model

In the case of independent multiple scattering, we can develop a statistical approach based on the geometrical description of photon trajectory. This approach uses classical concepts of statistical physics or polymer physics (gyration radius of a statistical coil or a fractal aggregate, persistence length). In the case of multiple light scattering, photons undergo a variable number of scattering events before escaping the medium. Furthermore, the extremities of the photon trajectory lie in a same plane. The photon trajectory in a granular medium is strongly influenced by the asymmetry parameter of the scattering centers. We consider the progressive deviation of a photon from the incident direction. In the ith scattering step, the photon progresses an average distance $\langle \cos\theta \rangle^i \lambda = g^i \lambda$ in the incident light direction. The average length $\xi(g)$ along the incident direction of the projected photon trajectory after many scattering events is:

$$\xi(g) \approx \sum_i \langle \cos\theta \rangle^i \lambda \approx \frac{\lambda}{1-g} \cdot \tag{9}$$

The characteristic distance $\xi(g)$ represents a decorrelation length or a persistence length above which the photon forgets both the direction of the incident beam and the scattering pattern of single particles. The persistence length $\xi(g)$ corresponds to an average number of the scattering events $X = 1/(1-g)$.

The photon trajectory can be assimilated to a random isotropic walk with average step equal to the persistence length $\xi(g)$. In first approximation, the minimal average exit distance D^* of the photons with respect to the center of backscattering spot scales as the persistence length $\xi(g)$. On the other hand, for each scattering event, the photon undergo an average angular deviation $\langle\theta\rangle = \arccos(g)$ from the incident direction. The photon backscattering thus requires a minimal average number of scattering N^* such as:

$$N^* \approx \frac{\pi}{\langle\theta\rangle} \approx \frac{\pi}{1-g} \cdot \tag{10}$$

A random trajectory of n steps of average length a presents an average gyration radius $r_G = an^{1/2}$. If n is sufficiently large, we can apply the central limit theorem and express the probability $P(r, n)$ to find the extremities of the trajectory at a distance r [8]:

$$P(r, n) = n^{-3/2} \mathrm{e}^{-\frac{3r^2}{\varepsilon n a^2}}, \tag{11}$$

with $\langle r \rangle = 0$ and $\varepsilon = 2$ for a volumic repartition of the extremities of the random walk trajectory. By assimilating the photon trajectory to an isotropic random walk of $N(1-g)$ elementary steps of average length $\xi(g)$, we then deduce an analytical expression for the backscattering probability $P(D, N)$ of photons at radial distance D after N scattering events:

$$P(D, N) = N^{-5/2}(1-g)^{1/2} \mathrm{e}^{-\frac{3D^2}{\varepsilon \langle D(N)\rangle^2}}$$
$$\text{with} \quad \langle D(N)\rangle = \lambda \left[\frac{N}{1-g}\right]^{1/2} \quad \text{and } \varepsilon = 4, \tag{12}$$

where $\langle D(N)\rangle$ represents the average exit distance of photons in the backscattering spot after N scattering events. The value $\varepsilon = 4$ results from the fact that the extremities of photon trajectory lie in the same plane (backscattering plane). The photon transport equation only involves the photon mean path length λ and the mean asymmetry factor g. For absorbing particles, we can introduce an absorption rate $\tau_A = \mathrm{e}^{-KN}$ of photons after N scattering events and express the photon exit probability $P(D, N)$ in the form:

$$P(D, N) = N^{-5/2}(1-g)^{1/2} \mathrm{e}^{-\frac{3D^2}{4\langle D(N)\rangle^2}} \mathrm{e}^{-KN}. \tag{13}$$

We have determined the photon exit probability $P(D, N)$ from numerical simulations for anisotropic scattering centers (Fig. 2). For long path photons with $N > 3N^*$ and $D > D^* = \pi\xi(g)$, the photon exit probability obeys a Gaussian statistic in agreement with the central limit theorem and the expression (11) derived from a statistical

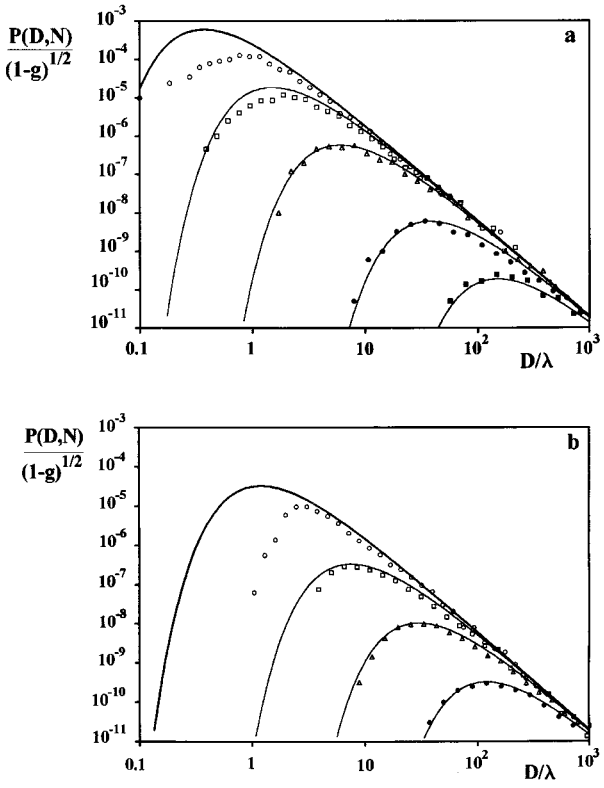

Fig. 2. Probability of photon backscattering $P(D,N)$ after n scattering events in a semi-infinite medium *versus* the reduced radial distance D/λ. Symbols were obtained from Monte-Carlo simulations and solid lines are calculated from equation (11). Curve (a): $g = 0.8$, $g_A = 0.8$, $g_B = -0.5$, $P_B = 0.23$ and $K = 0$ ((○) $D = 5\lambda$, (□) $D = 10\lambda$, (△) $D = 20\lambda$, (●) $D = 50\lambda$, (■) $D = 100\lambda$). Curve (b): $g = 0.9$, $P_B = 0$ and $K = 0$ ((○) $D = 20\lambda$, (□) $D = 50\lambda$, (△) $D = 100\lambda$, (●) $D = 200\lambda$).

model (Fig. 2). The distribution $Q(\theta)$ of backscattering angles further displays no dependence on the asymmetry factor for long path photons and obeys the relation:

$$Q(\theta) = \cos(\theta)^{3/2}. \tag{14}$$

Therefore, the scattering angle has no influence on the photon transport equation. On the other hand, the angular distribution $Q(\theta)$ and the density probability $P(D,N)$ of the short path photons ($N < 3N^*$) depends on the fine structure of the scattering diagram. Indeed, we observe an exclusion of short path photons from the center region of the backscattering spot ($D < \xi(g)$, Fig. 2) This phenomenon is accentuated by the anisotropy of the scattering diagram and the absence of backward scattering by particles (Fig. 2). The numerical simulations further confirm the exponential dependence of $P(D,N,g,K)$ with the absorption parameter.

4 Intensity profile in the back-scattered spot

The integration of the photon exit probability $P(D,N)$ over the scattering number N then yields the radial flux $F(D,g,K)$ per unit area in the backscattering spot:

$$F(D,g,K) = \frac{\displaystyle\int_{N=1}^{\infty} P(D,N)\mathrm{d}N}{\displaystyle\int_{N=1}^{\infty}\mathrm{d}N\int_{0}^{\infty} 2\pi D P(D,N)\mathrm{d}D}\cdot \tag{15}$$

A numerical integration of this equation leads to a radial dependence of the intensity $F(D)$ in agreement with computer simulations in the limit of a weak absorption of short path photons ($K < 1/N^*$). For $D > D^*$ and $K < 1/N^*$, we can then integrate the equations (11, 13) and derive an analytical expression for the area intensity $F(D)$ in the backscattered spot:

$$F(D) = \frac{D^{-3}}{\pi(1-g)}\mathrm{e}^{-DK^{1/2}(1-g)^{1/2}} \text{ for } D > D^*. \tag{16}$$

For non absorbing particles, the area intensity $F(D)$ at large distances thus scales as the radial distance power -3, due to the random nature of the light scattering process. However, the statistical model does not describe the center region of the backscattering spot relative to short path photons. The radial intensity $F(D)$ at small distance indeed increases with the backward scattering probability P_B and obeys a different statistic law depending on the fine structure of the phase function. Numerical simulations relative to real scatterers show that for a backward scattering probability $P_B > 5\%$, the area intensity $F(D)$ near the center of the backscattering spot ($D < D^*$) scales as the radial distance power -1.4 :

$$F(D,g,N) = \alpha(g,K)D^{-1.4}\mathrm{e}^{-DK^{1/2}(1-g)^{1/2}} \quad \text{for } D < D^*. \tag{17}$$

Equations (16, 17) describe the intensity profile in the whole backscattering spot in good agreement with the results from numerical simulations (Fig. 3).

5 Imagery analysis of the back-scattering spot image

In this section, we present a sizing optical technique based on the analysis of the two-dimensional backscattering spot image formed by the light scattered by a random gas/solid or liquid/solid dispersed medium.

We have developed an original imaging technique which allows a real time intensity of the backscattered spot image over more than 10^6 grey levels. We illuminate the granular medium with a collimated laser light and the we visualize the backscattering spot image with a CCD camera (XC77RRCE Sony) equipped with an electronic shutter (Fig. 4). The method consists in saving several images under variable shutter speed so that we can explore the different brightness regions of the backscatted spot image (Fig. 5). The electronic shutter of the camera is controlled in real time through TTL signals delivered by a DT2817 card (Data Translation) located in a microcomputer (Fig. 1). The treatment of the images then gives

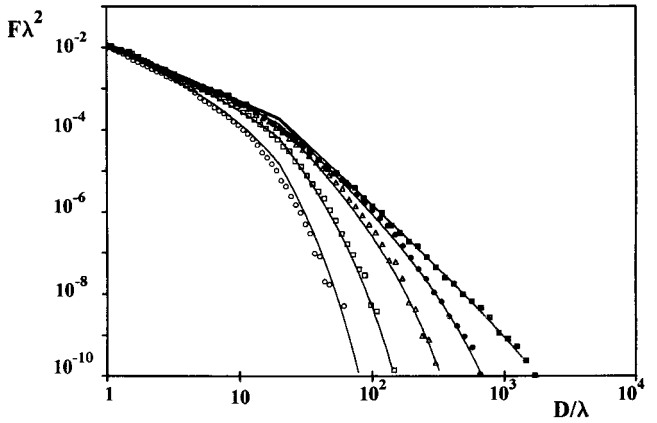

Fig. 3. Reduced radial intensity profiles $F(D/\lambda, K)\lambda^2$ in the backscattering spot derived from Monte-Carlo simulations for $g = 0.8$, $g_A = 0.95$, $g_B = -0.5$, $P_B = 0.10$, (□) $K = 10^{-6}$, (•) $K = 10^{-4}$, (△) $K = 10^{-3}$, (■) $K = 10^{-2}$ or (○) $K = 0.05$. The solid lines are calculated from the equations (14, 15) derived from the statistical model.

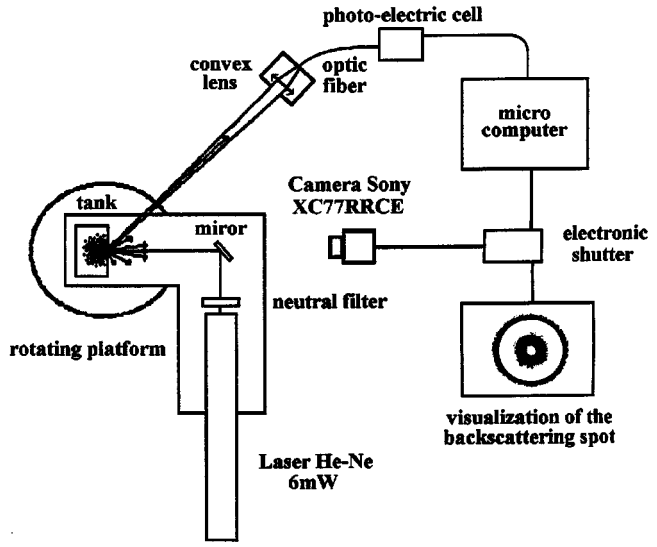

Fig. 4. Schematic representation of the experimental setup for the backscattering experiments.

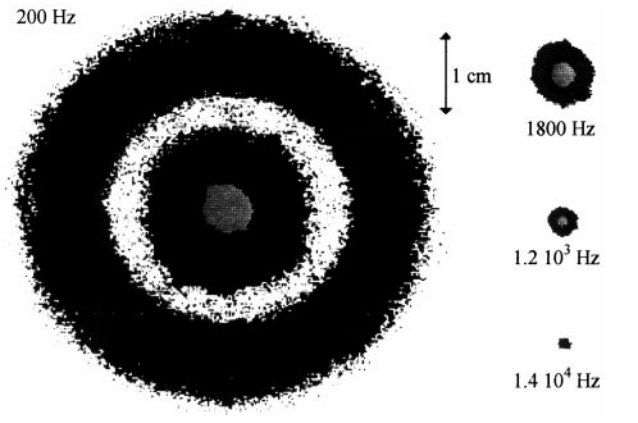

Fig. 5. Backscattering spot images for alumina particles in water ($d = 112$ μm, $\phi = 20\%$, scattering angle $\theta = 10^\circ$ and glass wall of thickness $V = 12$ mm) acquired at frequency video when varying the shutter speed.

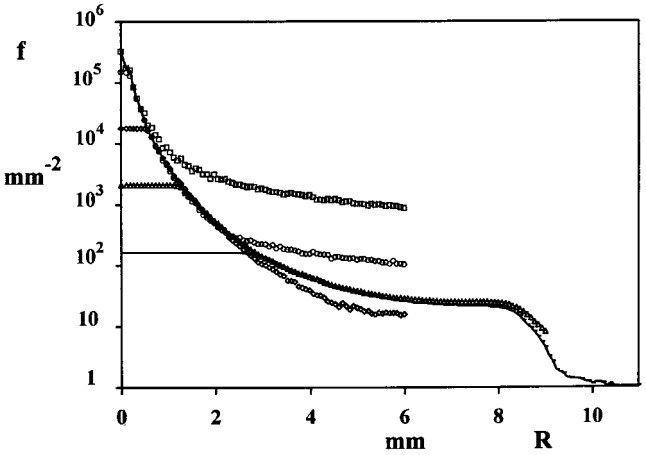

Fig. 6. Radial grey level profile $f(D)$ in the backscattering spot image (solid line) obtained from the analysis of five images acquired at variable shutter speed for alumina particles in air ($d = 90$ μm, $\phi = 60\%$, scattering angle $\theta = 10^\circ$ and glass wall of thickness $V = 5$ mm). Shutter speed $\Omega = 61145$ Hz (□), $\Omega = 7200$ Hz (○), $\Omega = 850$ Hz (△), $\Omega = 250$ Hz (▲) and $\Omega = 66$ Hz (–).

the grey level profile $f(D, \theta)$ in the backscattered spot (backscattering angle θ) over more than 10^6 grey levels (Fig. 6). The flux calibration of the imagery system performed with a non absorbing standard reflectance (Labsphere Inc.).

The area intensity profile $F(D)$ is then derived from the relation:

$$F(D) = \frac{Q_0(\theta)}{Q(\theta)} \frac{f(D,\theta)}{\displaystyle\int_0^\infty 2\pi D f_0(D,\theta) \mathrm{d}D} \tag{18}$$

where $Q(\theta)$ is the probability density of the backscattering angle θ and the subscript "0" refers to the non absorbing standard reflectance. Numerical simulations and measurements with a photo electric cell (Fig. 1) of the backscattered flux by a standard reflectance or a gas/solid suspension shows that the probability density of the backscattering angle θ obeys the general law [9,10]

$$Q(\theta) = Q_0(\theta) = \cos(\theta)^{3/2}. \tag{19}$$

In the case of liquid/solid, internal reflection and refraction of photons at the interface liquid/glass/air alters the distribution $Q(\theta)$ of the backscattering angle:

$$Q(\theta) = (\cos\theta_\mathrm{s})^{3/2} \frac{\tan\theta_\mathrm{s}}{\tan\theta} \quad \text{with} \quad \sin\theta = n_\mathrm{s} \sin\theta_\mathrm{s} \tag{20}$$

where n_s is the refractive index of the liquid phase and θ_s the photon incidence in the suspension (the distribution of the scattering angles in the suspension is $(\cos\theta_\mathrm{s}^{3/2})$. After an internal reflection on the outer surface of the glass wall, the photon turns back in the suspension and exits at a larger radial distance. The internal reflections at

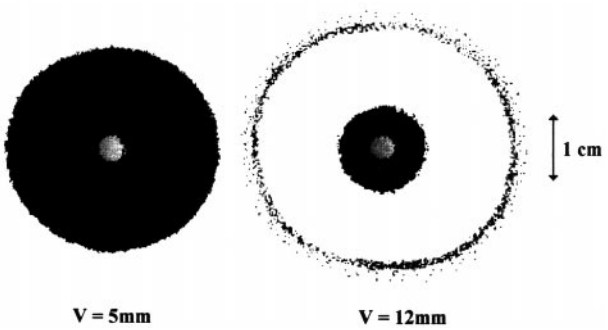

Fig. 7. Influence of thickness of glass wall on the backscattering spot image for alumina particles in water ($d = 112$ μm, $\phi = 10\%$, scattering angle $\theta = 10°$, shutter speed $\Omega = 66$ Hz and glass wall of thickness $V = 5$ mm or $V = 12$ mm).

the interface glass/air thus give rise to a light ring in the backscattered spot image [11,12] (Fig. 7). The radius r_0 of the light ring increases linearly with the thickness V of the glass wall and the photon deviation after an internal reflection ($r_0 = 1.85$ V) [11,12]. This phenomenon consequently alters the outer region of the backscattering spot. Therefore, we use a thick glass wall for pushing away the light ring ($V = 12$ mm, Fig. 7) which no longer influences the center part of the backscattering spot. However, the internal reflections reduce the area intensity in the backscattered spot. We then introduce the reflection coefficient B of the photons at the outer interface glass/air and we define the corrected area intensity $F(D)$:

$$F(D) = \frac{1}{1-B}\frac{Q_0(\theta)}{Q(\theta)}\frac{f(D,\theta)}{\displaystyle\int_0^\infty 2\pi D f_0(D,\theta)\mathrm{d}D}\cdot \qquad (21)$$

Using the Fresnel formula and considering a distribution $(\cos\theta_s)^{3/2}$ for the backscattering angles in the suspension, we have determined the analytical expression for the reflection coefficient $B(n_s)$ [11,12]. The reflection coefficient B increases with the reactive index of the liquid phase in very good agreement with the results from the numerical simulations (Fig. 8) and may reach 40% for particles suspended in water. Now, we may directly compare the experimental area intensity given by (21) with the results from the statistical model or from the numerical simulations.

6 Experimental analysis of the back-scattering spot

Scattering experiments were performed with sieved alumina particles (mean diameter 90 μm or 112 μm) suspended in water. Figure 9 shows the backscattering spot images for different particle volume fractions (shutter speed $\Omega = 92$ Hz, glass wall of thickness $V = 12$ mm).

We have used the relation (21) for the analysis of the images and the determination of the experimental radial dependence of the area intensity $F(D)$ (Fig. 10a). In the center region of the backscattering spot, the area intensity

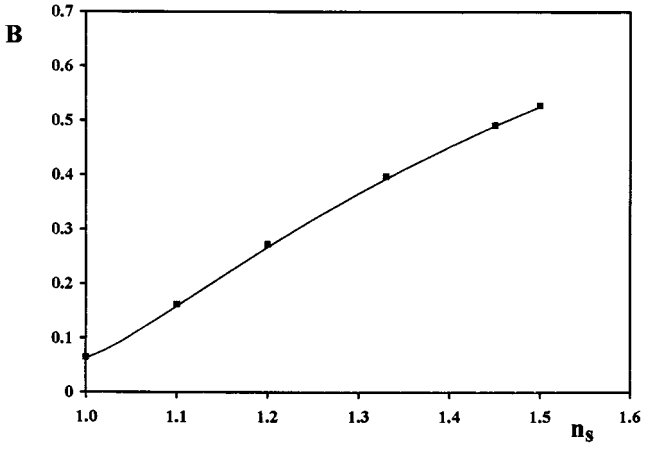

Fig. 8. Reflection coefficient B of the backscattered photons on the outer surface of the glass wall *versus* the refractive index of the suspending liquid. Squares (■) are obtained from numerical simulations and the solid line is derived from the Fresnel formula by considering the angular distribution $Q(\theta) = (\cos\theta)^{3/2}$ for the backscattered photons.

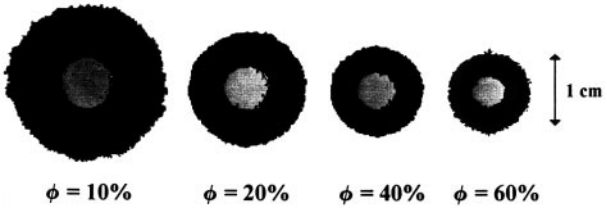

Fig. 9. Influence of the particle volume fraction on the backscattering spot image for alumina particles in water ($d = 112$ μm, scattering angle $\theta = 10°$, shutter speed $\Omega = 92$ Hz, glass wall of thickness $V = 12$ mm and particle volume fraction $\phi = 10\%$, $\phi = 20\%$, $\phi = 40\%$ and $\phi = 60\%$).

$F(D)$ increases with particle volume fraction. As a consequence, the size of the backscattering spot decreases with a particle volume fraction because of the invariance of the diffuse reflectance of optically thick suspensions. By introducing the photon mean path length $\lambda = d/3\phi$, we have plotted the dimensionless intensity $F\lambda^2$ *versus* the reduced radial distance D/λ. Then we get a single curve without dependence on the particle volume fraction (Fig. 10b). This curve displays two regions relative to short or long path photons in agreement with the theoretical developments and points out the independent character of light scattering by large particles.

As a first approximation, light scattering may be considered as independent even for a random packing of alumina particles ($\phi = 60\%$) despite the close contact of scattering centers. This result agrees with recent works from De Tien (1994) showing that the transition between dependent and independent scattering occurs for a particle volume fraction of about 70% in the case of a size parameter $A = 100$. The analytical expressions (16, 17), derived from the statistical model correctly describe the variations of the reduce intensity $F\lambda^2$ for an asymmetry factor $g = 0.75$ and an absorption parameter $K = 10^{-4}$

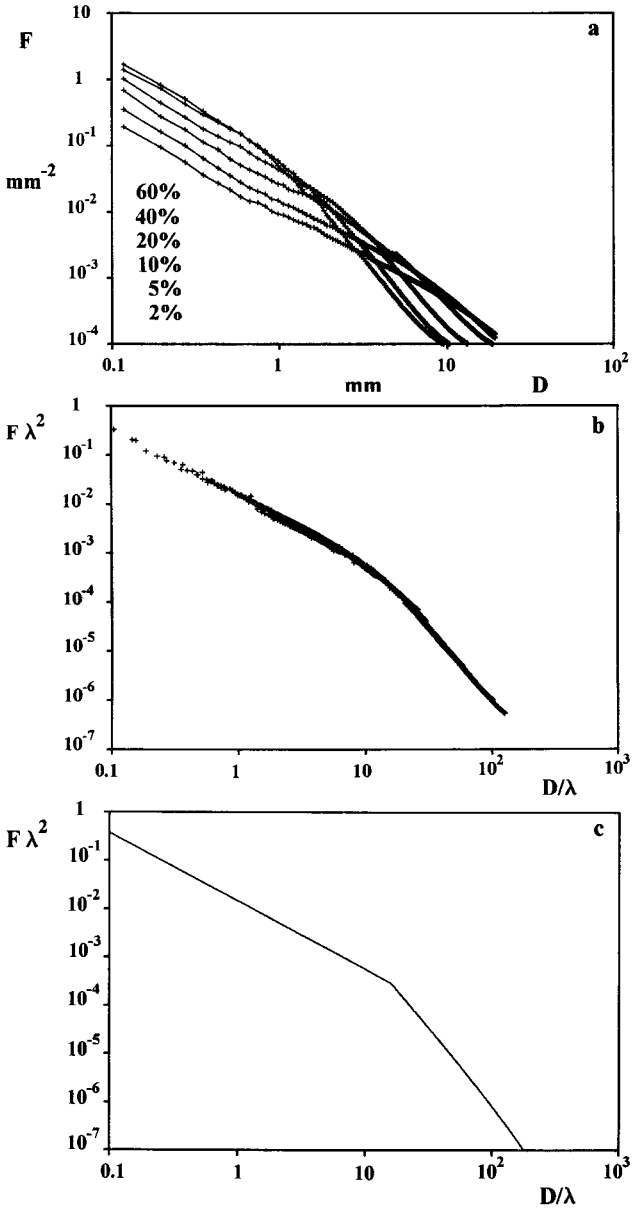

Fig. 10. Intensity profile $F(D)$ in the backscattering spot for alumina particles in water and various particle volume fraction ($d = 112$ μm, scattering angle $\theta = 10^\circ$, glass wall of thickness $V = 12$ mm, $\phi = 2\%$, $\phi = 5\%$, $\phi = 10\%$, $\phi = 20\%$, $\phi = 40\%$ and $\phi = 60\%$). Curve (b) shows the experimental data $F(D/\lambda)\lambda^2$ in a dimensionless form and curve (c) displays the theoretical dependence $F(D/\lambda)\lambda^2$ derived from equations (14, 15) with $g = 0.75$ and $K = 3 \times 10^{-4}$, $Q(\theta) = (\cos\theta)^{3/2}$.

(Fig. 10). Figure 10c displays the theoretical dependence $F(D/\lambda)\lambda^2$ derived from equations (14, 15) with $g = 0.75$ and $K = 3 \times 10^{-4}$.

7 Conclusion

Within the purpose of understanding the radiative transfer in granular media, we have developed statistical models which only involves a few physical parameters: the photon mean path length scaling as the inverse of particle area per unit volume, the mean asymmetry factor g describing angular scattering by individual particles in forward and backward directions, and the absorption probability of photon between two scattering events. We have introduced a persistence length or transport length for describing the progressive deviation of light from the incident direction. The renormalization of the photon trajectory then leads to an analytical expression for the backscattering probability of photons at radial distance D after N scattering events. Statistical models together with numerical simulations lead to a simple analytical expression for the radial dependence of the area intensity in the backscattering spot. The backscattering spot displays two regions: the center region relative to short path photons in which the flux decreases with photon mean path length and the outer region relative to long path photon in which the light flux scales as the mean path length (diffusion approximation). The description of the center region of the backscattering spot (non asymptotic regime scattering) uses an free exponent. This exponent is well-determined when elementary particles scatter a significant part of the incident flux in backward direction ($P_B > 5\%$).

The experimental analysis of the backscattering spot images in liquid-solid or gas-solid suspensions confirms the scaling laws and allows to derive both the particle surface area per unit volume and the optical properties of scattering centers. The particle surface area is an important parameter which determines the local exchanges of mass and heat in multiphase reactors. Finally, the two-dimensional backscattering spot encloses more information than the mono-dimensional output signal from an optic fiber sensor and thus provides a powerful way for the direct evaluation of the dispersed phase properties.

References

1. J. Werther, E.U. Hartege, D. Rensner, *Measurent techniques for gaz/solid fluidized bed reactors* (Lavoisier, 1991), pp. 1–17.
2. L. Rizzuti, P.L. Yue, Chem. Eng. Sci. **38**, 1241 (1983).
3. H.C. van de Hulst, *Multiple light scattering* (Acad. Press. New York 1980), Vol. 1 and 2.
4. C. Borhen, D.R. Huffman, *Absorption and scattering of light by small particles* (John Wiley and sons, 1983).
5. P.E. Wolf, G. Maret, Phys. Rev. Lett. **55**, 2696 (1985).
6. P. Mills, P. Snabre, Eur. Phys. Lett. **25**, 651 (1994).
7. A.H. Gandjbakhche, P. Mills, P. Snabre, Appl. Opt. **33**, 1070 (1994).
8. P.-G. de Gennes, *Scaling concept in polymer physics*, 2nd edn. (Cornell Univ. Press, 1987).
9. P. Snabre, Ph.D. thesis, University Paris VII, 1989.
10. A. Arhaliass, Ph.D. thesis, Institut National Polytechnique, Toulouse, 1994.
11. A. Arhaliass, P. Snabre, *Diffusion multiple de la lumière par les suspensions concentrées. caractérisation des milieux granulaires par analyse de la tache de rétrodiffusion* (Lavoisier, 1995), pp. 43-51.
12. A. Arhaliass, P. Snabre, ASME Heat Transfer and Fluids Eng., N° H01037, pp. 511–518, 1995.